

NUMERICAL ANALYSIS OF AERODYNAMIC CHARACTERISTICS OF HANG GLIDER

Don P Jose and Tide P S

School of Engineering, Cochin University of Science and Technology, Cochin-22, Kerala, India.

Abstract

The analysis of hang glider wing involves low speed aerodynamics during flight. The main focus of this work is to investigate the influence of multiple winglets on the climbing performance of hang glider. The hang glider with different configurations is numerically simulated using ANSYS CFD. Variation of sweep angles (15° , 20° and 25°) and dihedral angles (5° , 10° and 15°) are taken into consideration for the optimization of hang glider. A sweep angle of 15° and a dihedral angle of 10° gave higher coefficient of lift C_L compared to the other angles. An improvement in coefficient of lift is observed for wings with multiple winglets varying from 1 to 6.

Nomenclature

C_L = Coefficient of lift

C_D = Coefficient of drag

α = Angle of attack

1. Introduction

Hang gliding is one of the interesting aero sport in the twenty first century. It has developed into a practical sport, where the wings are built by aluminum and carbon fibre materials. Hang glider pilots are suspended by a special harness and launch from hills facing into wind.

. Unlike conventional aircraft, where the pilot can use aerodynamic control surfaces such as rudders, elevators, ailerons, etc., to change yaw, pitch and roll, a hang glider pilot cannot do it, since such features

do not exist on hang gliders. Instead the pilot has to shift the centre of gravity (CG) of the vehicle to perform such operations.

Hang gliding represents a kind of backyard technology and depends mainly on cut and try experimentation, the results are interesting on a range of technical levels. Whitcomb (1976) conducted a wind-tunnel experiment at high subsonic speeds of winglets fixed on the end of a first-generation wing. The magnitude of the increase in overall performance improvement provided by inclusion of the winglets.

Tucker (1993) conducted aerodynamic analysis of wing tip slots of gliding birds. The feathers in the bird's wing are similar to the winglets used on the wing tips of aircraft to reduce induced drag.

Huang (2006) conducted aerodynamic analysis with XFOil and LinAir Pro. The values of coefficient of lift and drag obtained from above two methods were compared. Zhidong (2012) reported an improvement in coefficient of lift after the introduction of winglets, panels and control surfaces.

In this present work, different sweep and dihedral angles are analyzed with same boundary conditions initially. The model with high coefficient of lift is taken for the subsequent analysis. The same model is later used to compare the performance of hang glider with different number of winglets.

2. Problem description and solution methodology

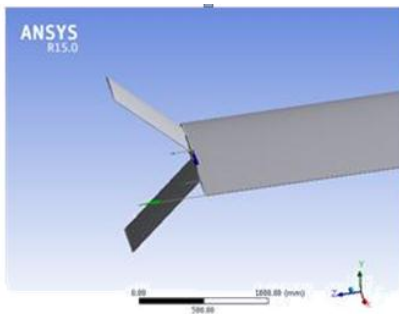


Fig.1 Hang glider with 2 winglets

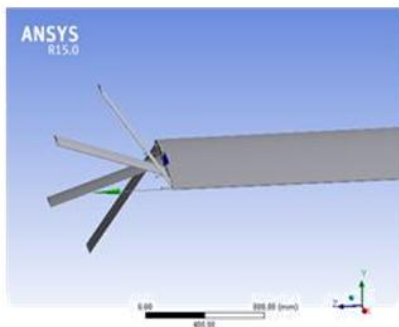


Fig. 2 Hang glider with 4 winglets

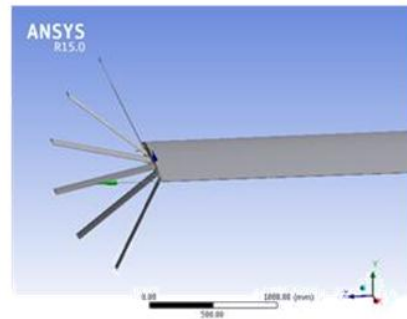


Fig. 3 Hang glider with 6 winglets

Hang glider with 2, 4 and 6 winglets are shown in Figures 1, 2 and 3 respectively. Different airfoils are used at the tip and the root of the wing. The root and tip airfoil is plotted with the help of airfoil plotter software. The dimensional details of the wing root airfoil are as follows:

Maximum thickness: 0.064 at $x/c=0.08$,
 Maximum camber: 0.019 at $x/c=0.06$,

The dimensional details of wing tip airfoil are as follows:

Maximum thickness: 0.060 at $x/c=0.3$,
 Maximum camber: 0 at $x/c=0$

Span	Surface Area	Mean aerodynamic chord	b^2/S
10.62m	18.780m ²	1.935 m	6.0
Swept angle	Taper ratio	Empty weight	Gross weight
35 ⁰	0.21	38 kg	90-150 kg

Table 1: Dimensions of hang glider symmetrical wing model

A pressure based turbulent solver was used for the numerical simulation. Hang gliders usually run at a speed ranging from 8 m/s to 35 m/s. In the present simulation the gliding speed is limited to 20 m/s. As the geometry of the model is scaled with a factor of 11.2, velocity of the flow is determined by matching the Reynolds number of both the scaled model and prototype. As such, the x component velocity of 224 m/s is applied at the inlet of the domain and outlet is maintained at constant atmospheric pressure. Shear Stress Transport $k-\omega$ turbulence model is used for solving the RANS equations..

3. Results and Discussions

Variation of coefficient of lift for different angles of attack is plotted in Figure 4. It is evident that as the number of winglets increases, an increase in the coefficient of lift is observed from the graph. But the improvement is visible only up to four winglets. A change in trend at high angle of attack is seen for six winglets.

Variation of coefficient of drag C_D for different angles of attack is shown in Figure 5. As angle of attack increases, coefficient of drag increases for all the models considered. As the number of winglets increases, coefficient of drag decreases and the value is a minimum for six winglets.

Pressure contours of double winglet and four winglet configurations are shown in Figures 6 to 13. A high pressure region is formed in the bottom part of the hang glider and low pressure region is formed on the upper regions of the hang glider. Lift is

formed due to the motion of air from higher pressure region to lower pressure region.

During the motion of air from lower surface to upper surface vortices are formed at the tip of the wing. Due to the presence of winglets, it breaks down the vortices formed at the tip of the wing. Due to the vortex breakdown, the coefficient of lift increases for the 4 winglet configuration.

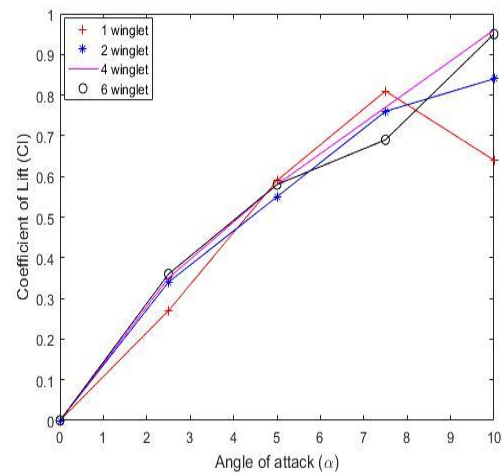


Figure 4 Variation of coefficient of lift at different angle of attack.

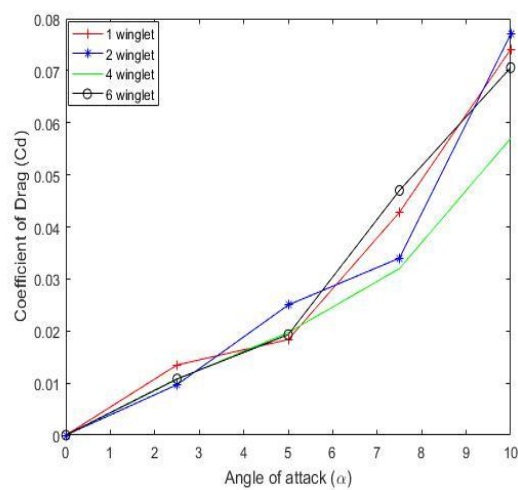


Figure 5 Variation of coefficient of drag at different angle of attack

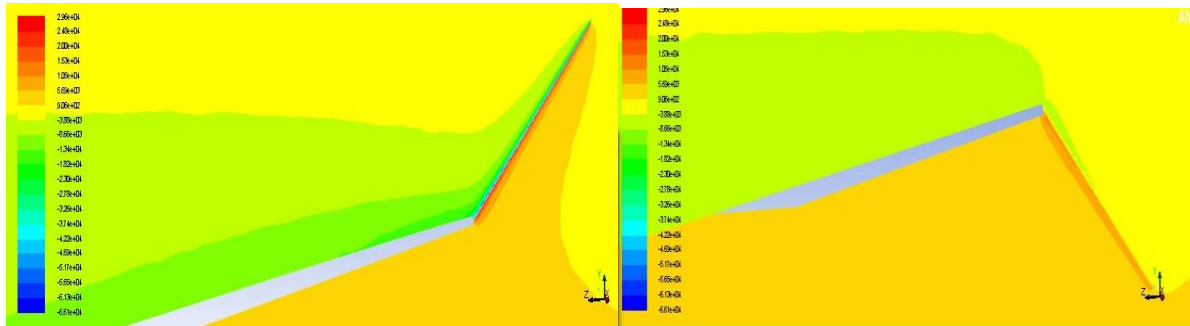


Figure 6: Pressure contours of double winglet at $\alpha = 2.5^\circ$

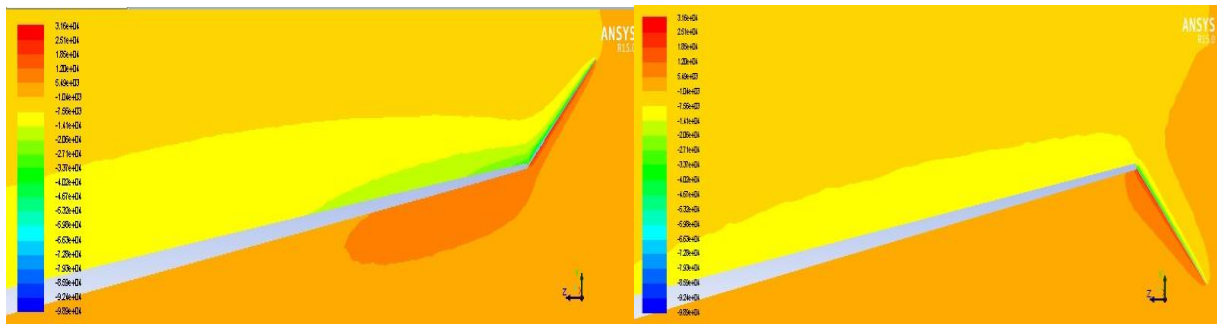


Figure 7: Pressure contours of double winglet at $\alpha = 5^\circ$

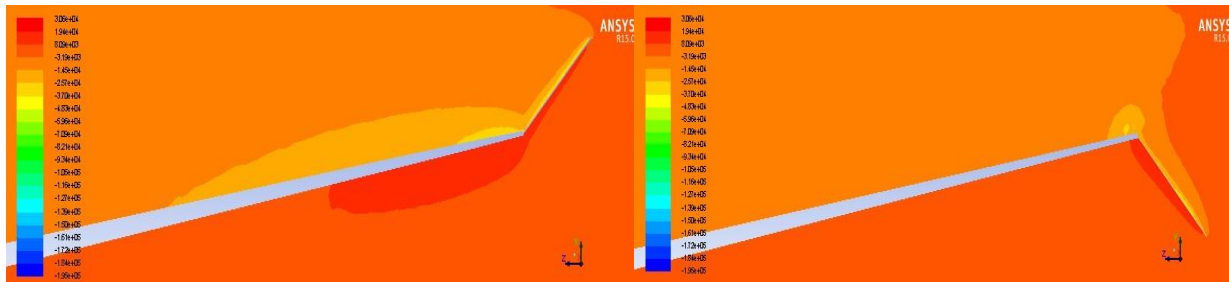


Figure 8: Pressure contours of double winglet at $\alpha = 7.5^\circ$

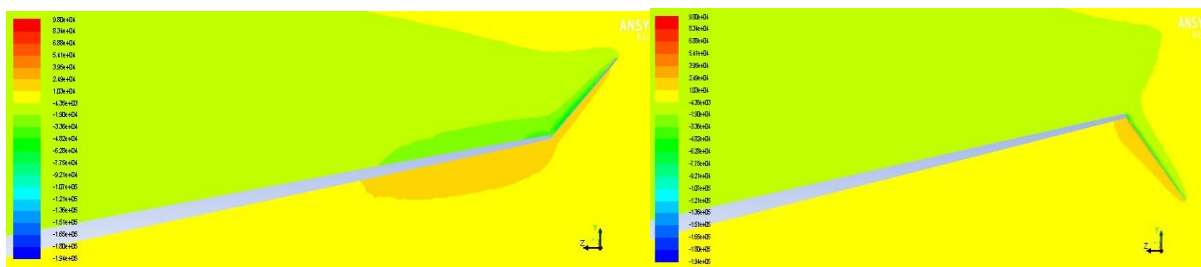


Figure 9: Pressure contours of double winglet at $\alpha = 10^\circ$



Figure 10: Pressure contours of four winglets at $\alpha = 2.5^\circ$

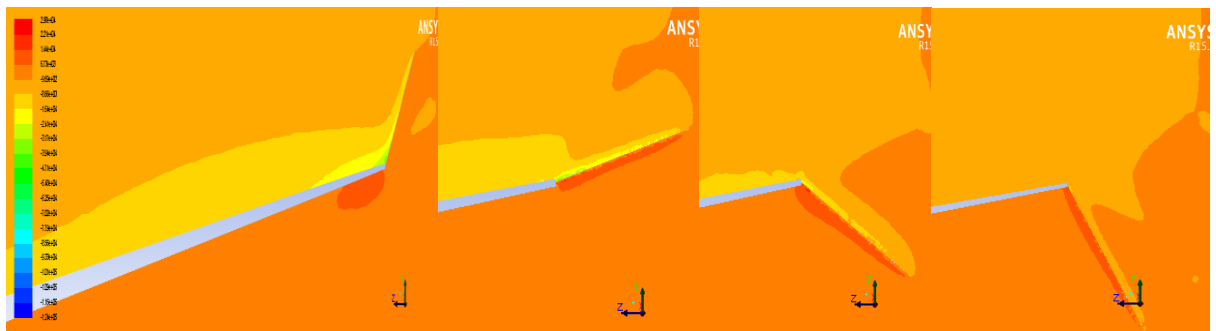


Figure 11: Pressure contours of four winglets at $\alpha = 5^\circ$

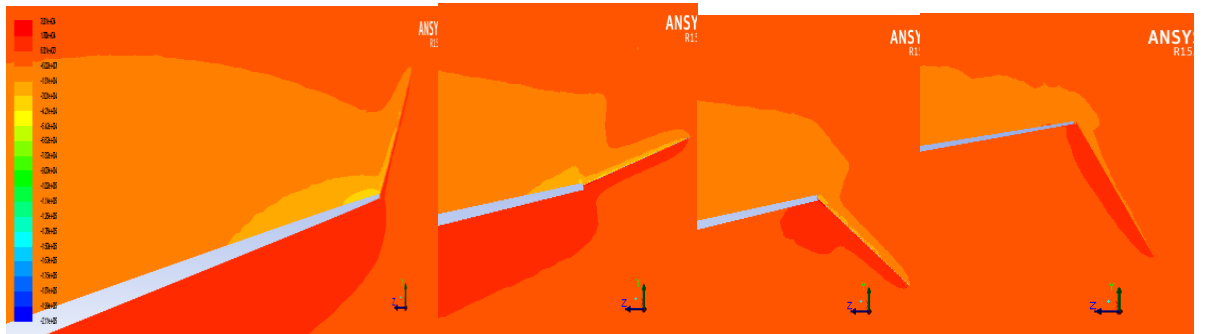


Figure 12: Pressure contours of four winglets at $\alpha = 7.5^\circ$



Figure 13: Pressure contours of four winglets at $\alpha = 10^\circ$

4. Conclusion

Aerodynamic analysis of hang glider models were carried out using ANSYS CFD. Coefficient of lift and drag were calculated for all the winglet configurations. It is evident that, as the number winglet increases coefficient of lift increases, especially at low values of angles of attack. Obviously, the value of coefficient of drag decreases with increase in number of winglets. Hang glider with four winglets showed better coefficient of lift at all values of angle of attack when compared with the other configurations. The improvement in coefficient of lift is due to the reduction of vortex formed at the tip of the wing. The presence of winglet enhances vortex breakdown and in turn reduces the strength of the vortex formed at the tip of the wing.

Acknowledgement

The author would like to thank all the reviewers for their suggestions.

References

- [1] Zhidong Fu. 2012 Aerodynamic analysis and design optimization. *AIAA*. 1074-1092.
- [2] Huang X. 2006 Aerodynamic analysis of a Class II high performance Hang Glider. 44th *AIAA* Aerospace sciences meeting and Exhibit, Reno 2006-446.
- [3] Whitcomb R. 1976. A design approach and selected wind tunnel results at high subsonic speeds wing-tip mounted winglets. *NASA Technical Note* 8260.
- [4] Tucker V.A. 1993 Gliding birds:Reduction of Induced drag by wing tip slots between the primary feathers. *Journal Of Experimental Biology* 180,285-310.